Investigation of scatter radiation of non-circular X-ray scan trajectories

Khanlian Chung, Lennart Karstensen, Marius Siegfarth, Lothar R. Schad, and Frank G. Zöllner

Khanlian Chung, Lothar R. Schad, Frank G. Zöllner
Computer Assisted Clinical Medicine
Medical Faculty Mannheim, Heidelberg University
Mannheim, Germany
khanlian.chung@medma.uni-heidelberg.de

Lennart Karstensen, Marius Siegfarth
Project Group for Automation in Medicine and Biotechnology
Fraunhofer Institute for Manufacturing Engineering and Automation
Mannheim, Germany

***Abstract*—Modern interventional X-ray devices are highly maneuverable and allow complex 3D imaging trajectories. New scan trajectories enable not only optimized object sampling but also introduce new approaches for dynamic 3D imaging. In this paper, we investigated the scatter radiation of two different scan trajectories. The scatter radiation was sampled by a rail setup with dosimeters at defined positions. After data analysis, contour maps were generated which show for four exemplary heights the scatter radiation distribution. The alternative scan trajectory showed smaller dose exposures at heights correlated to upper torso and head areas of a model physician.**

Keywords—Image acquisition, alternative scan trajectory, circular tomosynthesis, scatter radiation distribution

I. Introduction

In clinical routine, a variety of x-ray devices is used. Cone Beam Computed Tomography-devices (CBCT) support radiologists in interventional scenarios. Mounted on an industrial robot, these systems are highly maneuverable and allow for fluoroscopies from almost every angle and position. 3D imaging is possible as well.

Clinicians have to take extensive measures to protect themselves from scatter radiation. Therefore, low dose imaging is one of the most important recent research fields in the X-ray community. One way to reduce dose is to use task-based scan trajectories. Alternative trajectories enable more efficient ways to sample objects, resulting in better image quality or lower dose exposures [1–3]. Using new trajectories also means that the scatter radiation distribution is altered. Advantageous acquisition geometries would yield areas of little dose exposures. This would allow the clinician to remain in the intervention room and to optimize their workflow.

In this paper, we investigated the scatter radiation characteristics for two different scan trajectories: A standard CBCT was compared to a circular tomosynthesis scan trajectory [4]. Scatter radiations maps were generated to determine the dose exposure of medical staff.

II. Scan Trajectories

In this chapter, the two examined scan trajectories are explained. A Cartesian coordinate system as depicted in Fig. 1 was used. The x-axis is perpendicular to the X-ray source/detector axis and runs along longitudinal axis of the patient table. The z-axis is perpendicular to the patient table.

A. Cone Beam Computed Tomography (CBCT)

CBCTs can provide 3D isotropic images. A modern interventional X-ray device consists of a Cone Beam X-ray source with a flat panel detector (C-Arm) mounted on an industrial robotic system. It is possible to maneuver the C-Arm around the patient to take radiographs or projections for CBCTs. Conventional CBCT rely on analytical reconstruction techniques such as the Feldkamp-algorithm [5].

The reconstruction algorithms are based on the assumption that the X-ray device performed a simple planar circular scan trajectory (see Fig. 1 a)). Any detector and source movements can be described by a rotation matrix about the x-axis and is restricted to the y-z-plane.

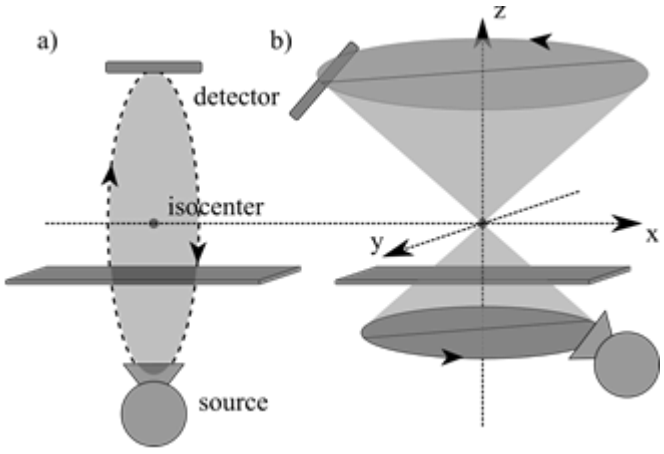

Fig. 1: Scan trajectories: (a) standard CBCT, (b) circular scan trajectory with the defined Cartesian coordinate system

DOI: 10.12059/Fully3D.2017-11-3202036

B. *Tomosynthesis*

In tomosynthesis techniques information and image quality are not uniformly distributed [6]. The scan trajectory determines the image quality distribution. For this paper, we chose a circular tomosynthesis scan trajectory [4] (Fig. 1 b)). In contrast to CBCTs, two rotation axes are required. Detector and X-ray source are tilted against the rotation axis z about the aperture angle at first. Subsequently, the C-Arm is rotated around the z-axis.

III. Image Quality Discussion

Circular tomosynthesis is similar to rotation laminography scan trajectories which are used in material science. Therefore, both can be discussed equally. Research groups have examined the impact of the aperture angle α in respect to image quality for rotation laminography [7, 8]. Due to the tilt of the C-arm against the rotation axis z, the distribution of information compared to conventional CT is alternated. Image quality is enhanced in x- and y-direction at the expense of the z-dimension. In k-space, the information distribution corresponds to the cylinder minus a symmetric double cone (Fig. 2). The perpendicular runs across k_z and the apex of the double cone is located the origin of the k-space. The half cone angle corresponds to the tilt angle $\vartheta = 90° - \alpha$. The lack of k-space information results in image artifacts similar to limited angle CT.

For comparison, Fig. 3 shows a simulated CT (100 projections), a simulated and a measured circular tomosynthesis ($\alpha = 25°$, 100 projections) of a calibration test phantom with 14 metal spheres. For all three settings, the same iterative reconstruction parameters were used.

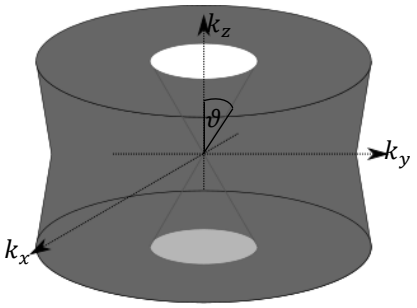

Fig. 2: k-space coverage of a circular tomosynthesis with missing information double cone [7, 8]

In the axial plane, the spheres are clearly visible in both CT and tomosynthesis techniques. On the one hand, ring artifacts when using tomosynthesis are apparent. On the other hand, the tomosynthesis methods show clearer edges compared to the CT. Also, the plastic cylinder of the phantom showed a better contrast.

In the sagittal plane, the spheres are blurred to ellipsoids in circular tomosynthesis due to the lack of information in k direction. Because the low frequencies are less affected by the missing double cone, depth information in z-direction is still available. In our comparison, all circle center positions showed a good match regardless of the scan trajectory.

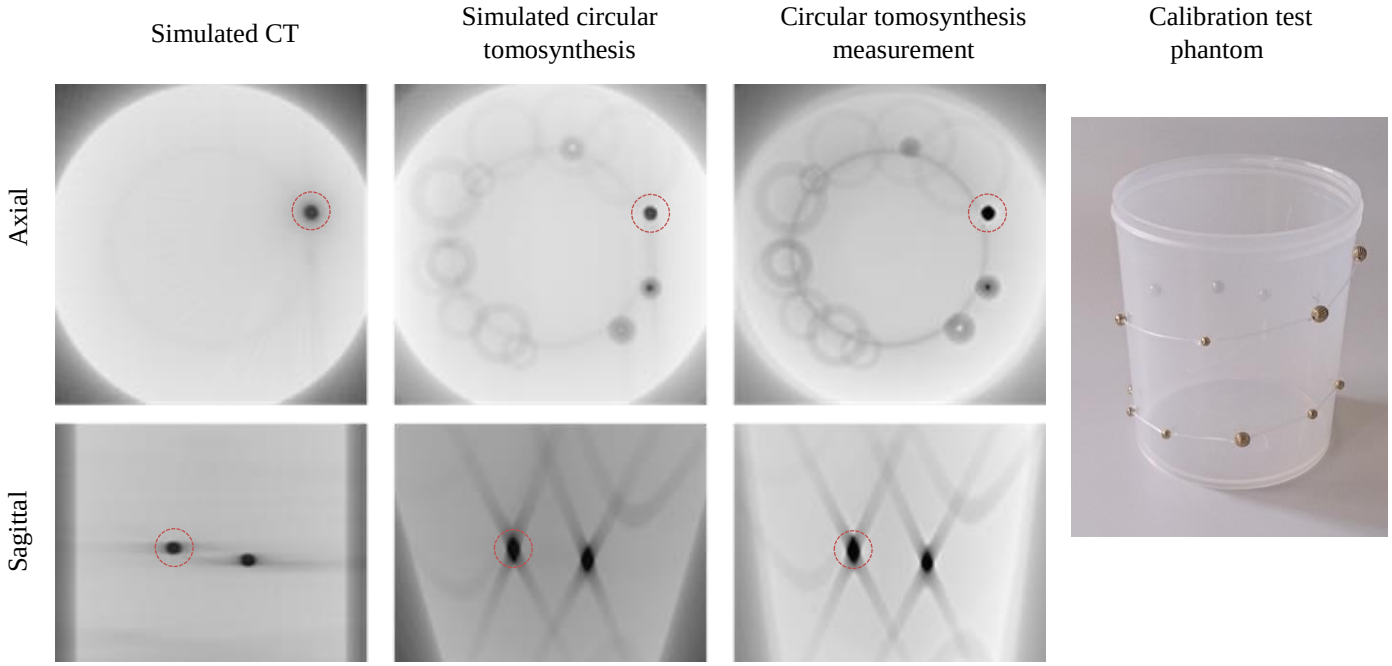

Fig. 2: Comparison of simulated CT and circular tomosynthesis (simulated and measurement): first row displays the axial plane of a calibration phantom, the second row the sagittal. The red circles indicate corresponding metal spheres. On the right side, the calibration test phantom is shown.

a)

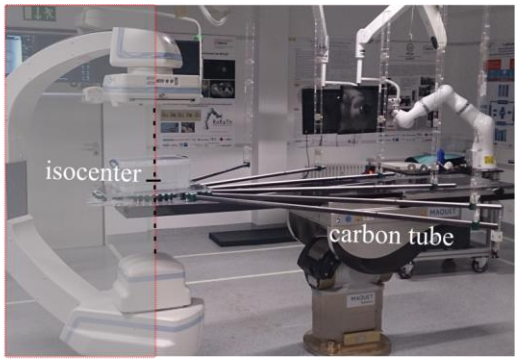

b)

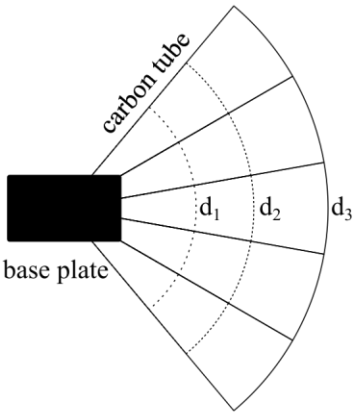

c)

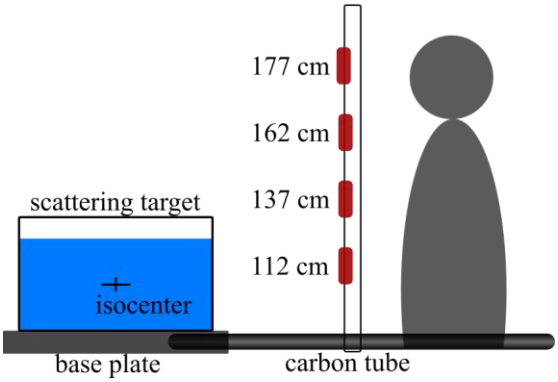

Fig. 4: Measurement setup, a) photography of the setup including neglected areas, b) rail system top view and c) schematic side view of the setup

IV. Experimental Setup

Our measurements were performed on a C-Arm CBCT (Artis Zeego, Siemens Healthineer, Forchheim, Germany). The setup is depicted in Fig. 4. It consists of a scattering target and a rail system for dosimeters.

We scanned the area right to the isocenter of both scan trajectories above patient table level. The space left to the isocenter was occupied by robotic movements and was not considered and is highlighted in grey. The space below the patient table was excluded since this is typically shielded by X-ray protective aprons and thus, very little dose exposure to medical staff is expected.

To measure scatter radiation at defined positions, a rail system was used. Six carbon tubes were mounted circular equidistant to the z axis on a base plate (Fig. 4 b)). On each carbon tube, four dosimeters (RaySafe i2, RaySafe, Billdal, Sweden) at defined heights of 112 cm, 137 cm, 162 cm and 177 cm (in respect to the floor, Fig. 4 c)) were placed. These heights are associated with waist, upper body and head area of an exemplary human. The dosimeter frames were adjusted on the carbon tubes at distances between 52 cm to 162 cm away from the isocenter. In total, an area of over 100° and 110 cm was covered and sampled by 240 dosimeter positions.

A scattering target consisting of a box (length x width x height: 37 x 25 x 15 cm) filled with 9 liters of water was placed above the baseplate in the isocenter of both scan trajectories.

For reference an Artis Zeego “Head Scan”- protocol provided by the manufacturer was used. The CBCT scans are performed at 109 kVp and sampling 496 projections within 20 s. Furthermore, the protocol comprises an intelligent dose optimization algorithm for minimizing dose exposure.

Said reference CBCT scan trajectory was compared to a circular tomosynthesis scan trajectory featuring 50 projections and an aperture angle of 25°. The projections were acquired at 109 kVp, 245 mA and 15 ms each.

For each dosimeter position configuration a CBCT and tomosynthesis scan was performed. Therefore, all dosimeter positions were exposed to similar x-ray and scatter radiation circumstances.

After the measurement the data had to be prepared for analysis. Because the protocol parameters were different for CBCT and tomosynthesis, each data set was separately normalized. The highest measured dose exposure for each scan trajectory was defined as 100%. To complete the scatter radiation maps, the data sets were interpolated into a Cartesian coordinate system.

V. Results

Fig. 5 shows the obtained scatter radiation maps. All four heights were evaluated and displayed in separate diagrams. The color map ranges from red (100% highest accumulated dose during one scan) to green (no exposure at all). For guiding purposes isodose lines were drawn.

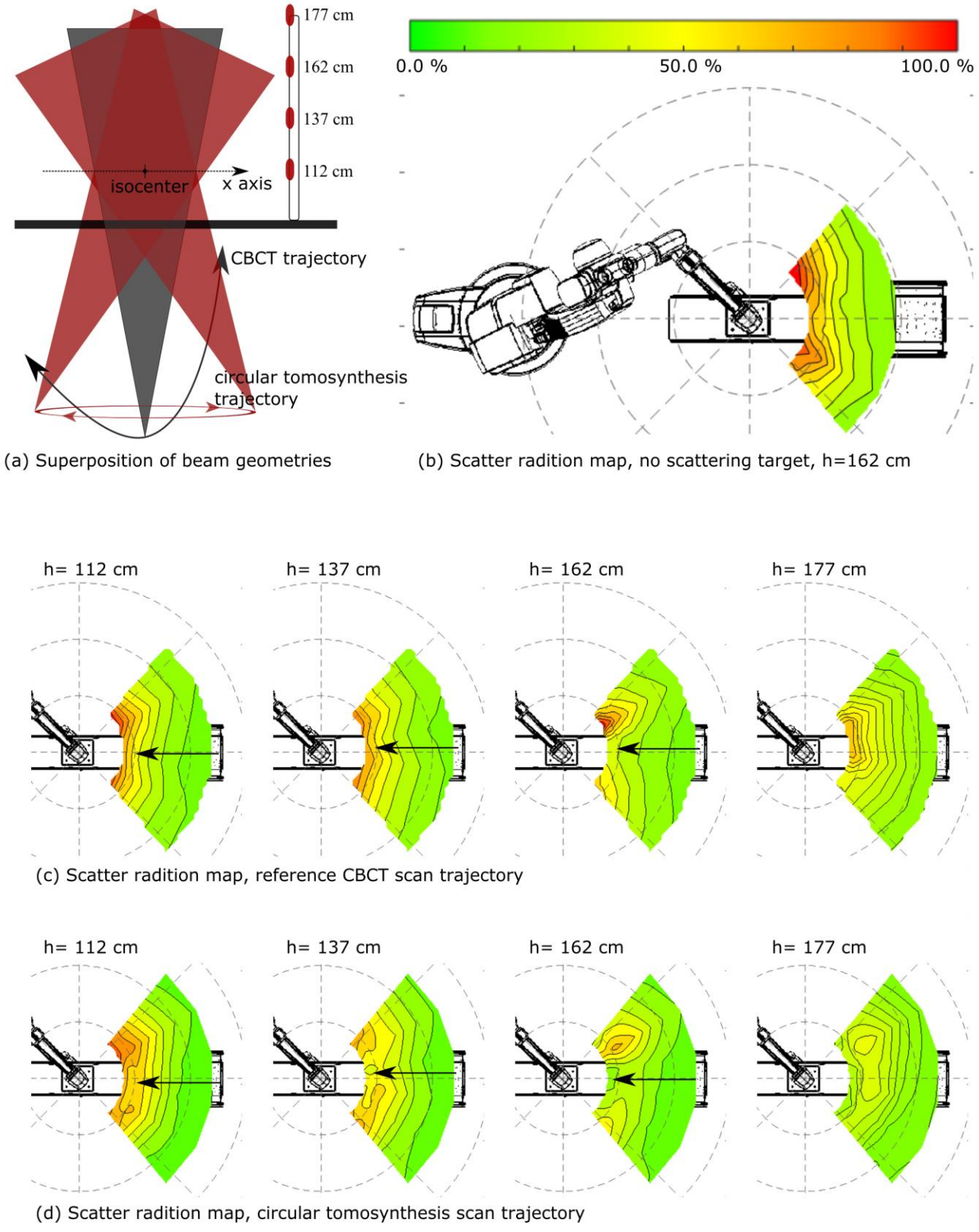

Fig. 5: Scatter radiation maps and superposition of scan trajectories:
(a) schematic geometrical superposition of the scan trajectories
(b) exemplary color map of scatter radiation measurement without a scattering target
(c) and (d) obtained scatter radiation maps for the two scan trajectories

The scatter radiation distributions of both trajectories display notches (marked by arrows in Fig. 5 (c) and (d)) in the isodose lines for every height. The measurements were repeated without a scattering target and yielded similar results (Fig. 5 (b)). The notches are not influenced by trajectory and are also visible in measurements without any scattering targets. Therefore, we assume it is caused systematically by the patient table.

For a height of 112 cm the tomosynthesis scan trajectory shows a higher dose exposure than the CBCT trajectory. Superposing all x-ray source and detector positions, circular tomosynthesis methods show wider beam extents around its isocenter (Fig. 5 (a)). Accordingly, we expected to detect a wider area exposed to scatter radiation at low heights.

With increasing height the tomosynthesis scan trajectory shows a qualitatively lower dose exposure. Especially for the upper torso and the face region the rates are lower. A standard CBCT scan performs typically a 180-200° arc starting from a horizontal position. During acquisition the C-Arm swings underneath the patient table to the opposite side, ending almost horizontal again. The more the C-Arm is tilted against the z-axis, the more horizontal is the imaging X-ray beam. This results in higher scatter radiations of our measured area.

In contrast, a circular tomosynthesis covers only a fraction of the rotation around the x-axis and the source remains below scatter target and patient table. Therefore, X-ray photons scattered at small or wide angles will irradiate floor and ceiling but not the measured area.

The highest dose values measured for the CBCT was 100% and 63% at a height of 162 cm and 177 cm. The tomosynthesis trajectory yielded 75% and 46% at the same heights.

VI. Conclusion

Our measurements showed differences in dose exposure for a reference CBCT and a circular tomosynthesis trajectory at an aperture angle of 25°. A tomosynthesis trajectory shows a wider distributed scatter radiation for the waist area. For face and upper torso region, dose exposure was lower than a standard CBCT trajectory. These areas are critical and exposed ones for medical staff [9].

Alternative scan trajectories allow for more complex task-based image acquisition. By taking scatter radiation into consideration, scan trajectories can be designed to minimize dose exposure in certain areas. If it is possible to reduce dose to a reasonable level, real-time 3D imaging would be feasible without forcing clinicians to leave the interventional room.

Acknowledgement

This research project is part of the Research Campus M^{2}OLIE and funded by the German Federal Ministry of Education and Research (BMBF) within the Framework “Forschungscampus: public-private partnership for Innovations” under the funding code 13GW0092D.

VII. References

[1] Hermann Schomberg (Hamburg) 4753 2001 Jan 16 14:15:42, “Complete Source Trajectories for C-Arm Systems and a Method for Coping with Truncated Cone-Beam Projections,”

[2] J. D. Pack, F. Noo, and H. Kudo, “Investigation of saddle trajectories for cardiac CT imaging in cone-beam geometry,” *Phys. Med. Biol.*, vol. 49, no. 11, pp. 2317–2336, 2004.

[3] K. Khare, B. E. H. Claus, and J. W. Eberhard, “Tomosynthesis imaging with 2D scanning trajectories,” in : SPIE, 2011, p. 796115.

[4] B. E. Claus, D. A. Langan, O. Al Assad, and X. Wang, “Circular tomosynthesis for neuro perfusion imaging on an interventional C-arm,” in : SPIE, 2015, 94122A.

[5] L. A. Feldkamp, L. C. Davis, and J. W. Kress, *Practical cone-beam algorithm*, vol. 1.

[6] J. T. D. Iii and D. J. Godfrey, “Digital x-ray tomosynthesis: current state of the art and clinical potential,” (en), *Phys. Med. Biol.*, vol. 48, no. 19, pp. R65, 2003.

[7] L. Helfen *et al.*, “High-resolution three-dimensional imaging of flat objects by synchrotron-radiation computed laminography,” *Appl. Phys. Lett.*, vol. 86, no. 7, p. 71915, 2005.

[8] F. Xu, L. Helfen, T. Baumbach, and H. Suhonen, “Comparison of image quality in computed laminography and tomography,” (eng), *Optics express*, vol. 20, no. 2, pp. 794–806, 2012.

[9] K. Chida *et al.*, “Occupational dose in interventional radiology procedures,” (eng), *AJR. American journal of roentgenology*, vol. 200, no. 1, pp. 138–141, 2013.